Sodium: A Charge-Transfer Insulator at High Pressures

Matteo Gatti,[1] Ilya V. Tokatly,[1,2] and Angel Rubio[1,3]

[1]*Nano-Bio Spectroscopy Group and ETSF Scientific Development Centre, Departamento Física de Materiales, Universidad del País Vasco, Centro de Física de Materiales CSIC-UPV/EHU-MPC and DIPC, Avenida Tolosa 72, E-20018 San Sebastián, Spain*

[2]*IKERBASQUE, Basque Foundation for Science, E-48011 Bilbao, Spain*

[3]*Fritz-Haber-Institut der Max-Planck-Gesellschaft, Theory Department, Faradayweg 4-6, D-14195 Berlin-Dahlem, Germany*

(Received 25 February 2010; published 27 May 2010)

By first-principles methods we analyze the optical response of transparent dense sodium as a function of applied pressure. We discover an unusual kind of charge-transfer exciton that proceeds from the interstitial distribution of valence electrons. The absorption spectrum is strongly anisotropic, which, just at pressures above the metal-insulator transition, manifests as sodium being optically transparent in one direction but reflective in the other. This result provides key information about the crystal structure of transparent sodium, a new unconventional inorganic electride.

DOI: 10.1103/PhysRevLett.104.216404 PACS numbers: 71.35.Cc, 61.50.Ks, 71.20.Dg, 78.40.−q

Simple-to-complex phase transition.—In textbooks sodium is defined as the simplest of the simple metals [1]. At ambient pressure it has a high-symmetry crystal structure with nondirectional metallic bondings. Valence electrons can be treated as almost independent particles, only weakly perturbed by the electron-ion interaction, forming a homogeneous and isotropic electron gas. As a consequence, the optical properties are also well described by the Drude model of free carriers. Application of pressure, instead, changes the situation quite dramatically while revealing an emergent complexity. Sodium under pressure shows an unexpected and often counterintuitive behavior. Instead of becoming more free-electron-like, at higher densities it adopts several low symmetry (and even incommensurate) crystal structures [2–7] and has a very unusual melting curve [4,8]. This surprising behavior had been anticipated by Neaton and Ashcroft [9], who also predicted a possible metal to insulator transition [10]. At very high pressures compression is sufficiently strong that core electrons start to overlap and the Pauli exclusion principle favors less symmetric charge distributions with *p-d* hybridizations [5,9]. The Coulomb repulsion between core and valence electrons leads to charge localization in interstitial positions, instead of around nuclei, and finally to an insulating state [9]. From a simple, uncorrelated, reflective metal, sodium turns into a complex, correlated, transparent insulator. It is a whole change of paradigm [11].

The crystal structure of the recently discovered insulating state was identified as a distorted, six-coordinated double-hexagonal closed-packed structure (*hP*4) [5]. Experimentally, it is found that under pressure body-centered cubic Na first becomes face-centered cubic (at 65 GPa) and then transforms into a *cI*16 structure [2] (at 103 GPa). Besides adopting many different structures near the minimum of the melting curve [3] (118 GPa), it crystallizes in the *oP*8 and *tI*19 phases [6] (above 125 GPa), before undergoing a final transition to the newly proposed *hP*4 phase at around 200 GPa. Theoretically [5], the transition occurs at slightly higher pressures (260 GPa). Measurements were performed at room temperature, while the zero-temperature structural calculations neglected entropic contributions and lattice dynamics (phonon enthalpies along with quantum effects on the light sodium ions), and hence could not provide a direct confirmation of the theoretical results [12].

In the present Letter, we study the optical response of the *hP*4 phase employing the highly accurate Bethe-Salpeter equation (BSE), which is the state-of-the-art approach for first-principles predictions of optical properties in solids [13]. Our results provide evidence for the emergence of relevant excitonic (i.e., electron-hole correlation) effects, with the formation of an unusual charge-transfer exciton, and a strong anisotropy in the dielectric response. They represent a stringent fingerprint of the *hP*4 crystal structure of transparent dense sodium.

Absorption spectra and excitons.—The BSE can be cast into an effective two-particle Schrödinger equation for the wave function $\Psi_\lambda(\mathbf{r}_h, \mathbf{r}_e)$ of the electron-hole pair (i.e., the exciton): $H_{\mathrm{exc}}\Psi_\lambda = E_\lambda\Psi_\lambda$, where the excitonic Hamiltonian H_{exc} includes the electron-hole interaction [13]. In our first-principles approach, Ψ_λ is represented on a Kohn-Sham basis: $\Psi_\lambda(\mathbf{r}_h, \mathbf{r}_e) = \sum_{\mathbf{k}vc} \Psi_\lambda^{\mathbf{k}vc} \phi^*_{v\mathbf{k}}(\mathbf{r}_h)\phi_{c\mathbf{k}}(\mathbf{r}_e)$, where v (c) runs on valence (conduction) bands and $\mathbf{k}$ is in the first Brillouin zone. The optical spectrum is then obtained from the imaginary part of the dielectric function $\epsilon_2 = \mathrm{Im}\,\epsilon$:

$$\epsilon_2(\omega) = \lim_{\mathbf{q}\to 0} \frac{8\pi}{q^2} \sum_\lambda \left| \sum_{\mathbf{k}vc} \Psi_\lambda^{\mathbf{k}vc} \langle \phi_{v\mathbf{k}+\mathbf{q}} | e^{-i\mathbf{q}\mathbf{r}} | \phi_{c\mathbf{k}} \rangle \right|^2 \times \delta(\omega - E_\lambda). \quad (1)$$

When excitonic effects are unimportant the eigenvalues E_λ

correspond to a vertical transition between one-quasiparticle energies $E_{c\mathbf{k}} - E_{v\mathbf{k}}$ (which we calculate in the *GW* approximation [14]) and the coefficients $\Psi_\lambda^{\mathbf{k}vc}$ become diagonal, reducing Eq. (1) to the well-known Fermi's golden rule [1]. We investigate the effect of pressure on the formation of excitons, through charge localization and the reduction of the screening of the electron-hole interaction. Excitons can be identified by means of the twofold role that they play on the absorption spectra. First, the modification of the excitation energies induces a shift of the positions of the peaks in the spectrum; as a consequence, new peaks can appear inside the fundamental band gap (bound excitons). Second, the mixing of the independent-particle transitions leads to a global reshaping of the spectrum towards lower energies (continuum excitons). Our *ab initio* solution of the BSE proceeds in three steps. We start from a ground-state calculation using density-functional theory in the local-density approximation (LDA), where we employ the lattice constants of the *hP*4 phase from Ref. [5] corresponding to representative pressures (see Ref. [15], Table 1). We treat 3*s*, 2*p*, and 2*s* explicitly as valence electrons, leaving only the very tightly bound 1*s* in the frozen ionic core (this required us to use an energy cutoff of 80 Ha in the plane-wave representation of the wave functions). We then calculate the quasiparticle *GW* electronic structure that we use as input for the Bethe-Salpeter equation. In the calculation of the screening and the *GW* corrections, where we adopt the Godby-Needs plasmon-pole model [16], we use 150 bands and a cutoff of 20 Ha on the wave functions. To converge the absorption spectra up to 7–8 eV we consider 2 valence and 8 conduction bands and sample the first Brillouin zone with a uniform grid of 2000 inequivalent **k** points, slightly shifted from high-symmetry **k** points. We apply a 0.1 eV Gaussian broadening [17].

Excitons in dense sodium.—To illustrate our discussion, we first consider the results obtained with the lattice parameters calculated by Ma *et al.* [5] in correspondence to a pressure of 320 GPa. We then analyze the dependence of the excitonic effects with applied pressure. In Fig. 1(a) we compare the absorption spectra that we obtain by solving the BSE or by using Fermi's golden rule (averaged with respect to the different light polarizations). In the latter case transition energies are calculated either using LDA or the *GW* approximation. The *GW* corrections on the band structure induce an almost rigid blueshift to the LDA spectrum, reflecting the correction of the usual underestimation of the quasiparticle band gap in LDA (see Ref. [15], Fig. 1). The onset moves from 1.7 eV in LDA to 3.0 eV in *GW*. It corresponds to a direct transition in Γ between the top valence and the bottom conduction bands. Adding interaction between *GW* quasiparticles, i.e., quasiparticle electron-hole attraction, we observe a substantial modification of the spectrum: (i) strong redistribution of the optical oscillator strength to lower energies, changing the global shape of the spectrum; (ii) strong narrowing of the main peak at ∼5 eV; and (iii) appearance of bound excitons inside the gap. It turns out that electron-hole attraction reduces the transition energies by about 0.1 eV, determining a global redshift of the joint density of states (JDOS) [inset of Fig. 1(a)]. The absorption onset is now at 2.9 eV [grey arrow in Fig. 1(a)]. This implies the formation of a bound exciton in the fundamental gap with a binding energy of about 100 meV, that is larger than the one obtained in standard semiconductors [13].

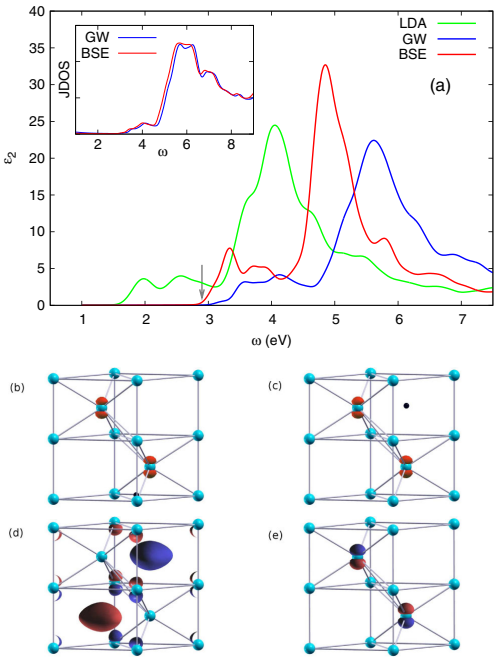

FIG. 1 (color online). (a) Absorption spectra calculated in different approximations (see text). The grey arrow marks the BSE onset. The inset shows *GW* JDOS vs density of excitonic states in BSE. (b)–(c) Isocontour plots of the electron-hole pair wave function $|\Psi_\lambda|^2$ at fixed $\mathbf{r}_h$ (black dot) for the first exciton at 0.3 of its maximum. (d) Kohn-Sham top valence and (e) bottom conduction wave functions at Γ: isocontours at +0.3 [red (light grey)] and −0.3 [blue (dark grey)] of their maximum.

In Figs. 1(b) and 1(c) we analyze the shape of the wave function corresponding to this bound electron-hole pair. We fix the position of the hole in a particular position $\mathbf{r}_h$ and determine the corresponding density distribution of the electron. Our calculation reveals that this bound exciton is, in particular, a charge-transfer exciton. While the hole is created in the vicinity of one corner atom [Fig. 1(b)], the excitation has largely moved the electron charge to localize on the central atoms, forming a separate sublattice over many unit cells (see Ref. [15], Fig. 2). Remarkably, the same electronic distribution is obtained even when the hole is located in the interstitial regions [Fig. 1(c)], where the valence electrons accumulate when they are forced away from the atoms [5,11]. Charge-transfer excitons are typical of ionic insulators like alkali-halide crystals [18]. They are intermediate between strongly bound Frenkel and weakly bound Wannier excitons, as they involve the transfer of one electron from a negative to a positive ion. In the present

case the role of the anion is played by the interstitially confined electron gas. In this sense, transparent sodium behaves as an unconventional inorganic electride [19], characterized by the simplest possible anion: an electronic charge without an ionic core. The strong enhancement of the peak at around 5 eV, which is the mark of the formation of a resonant exciton, is not explained by the simple modification of the transition energies, since the JDOS curves remain very similar. It is rather due to the mixing of a very large number of independent electron-hole transitions in the same energy range (see Ref. [15], Fig. 1), each of them participating with a small contribution to the excitonic peaks. This is a sign of highly correlated excitonic states.

Anisotropy and inhomogeneity.—By comparing the optical spectra obtained with light polarized either along the hexagonal c axis or in the perpendicular ab plane [Fig. 2(a)], we find that the spectra with the two light polarizations remain very different, both with and without the inclusion of excitonic effects. In particular, in the in-plane direction, sodium is completely transparent up to 4.5 eV. In fact, the absorption onset and the first structures in the spectrum in Fig. 1(a) are entirely due to absorption of light polarized along the c axis. Also, the exciton represented in Figs. 1(b) and 1(c) is dark in the in-plane direction. This behavior can be understood as due to the particular symmetry of the one-particle wave functions involved in the transitions. For instance, by symmetry at the Γ point the transition between the top valence [Fig. 1(d)] and the bottom conduction [Fig. 1(e)] has zero oscillator strength in the in-plane direction. On the other hand, inhomogeneities in the charge distributions are responsible for the so-called crystal local-field effects [20]. In general, an external field can induce spatial charge fluctuations that are rapidly varying on the microscopic scale. It is intuitively clear that the self-consistent response to these induced local fields becomes more important the more the system is inhomogeneous and polarizable. Whereas in the absorption spectra of bulk solids local fields are generally weak [13], in dense sodium they induce a sizable effect (see Ref. [15], Fig. 3), particularly for the main peak and c axis polarization. This is a further indication that the charge distribution has become very inhomogeneous.

Dependence on the pressure.—The application of increasing pressure induces as a first effect a band gap opening in the quasiparticle band structure [5]. As a consequence, the optical spectra also move to higher energies [Fig. 2(b)]. Moreover, the indirect quasiparticle gap becomes direct at the Γ point (see Ref. [15], Fig. 5). Additional compression leads to localizing the electronic charge more and reducing the screening of the interaction between the electron and the hole. Both contribute to increasing the excitonic effects: the electron and the hole, on average, stay closer and their effective interaction is stronger. This explains why the largest differences between the spectra with and without electron-hole interaction occur for the spectrum at the highest pressure [Fig. 2(b)]. In

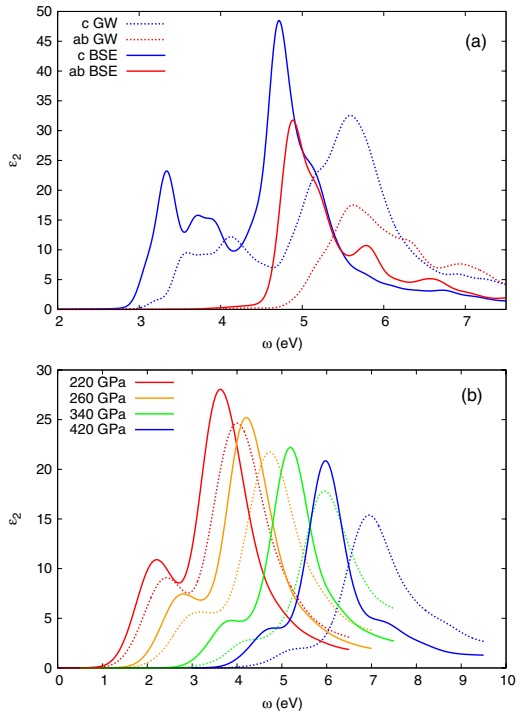

FIG. 2 (color online). (a) Spectra calculated with polarization either along the hexagonal c axis [blue (dark grey)] or in the in-plane ab directions [red (light grey)]. (b) Absorption spectra at increasing pressures, with or without excitonic effects (solid and dotted lines, respectively).

fact, the static dielectric constant, which we calculate in the random-phase approximation [13], decreases with increasing pressure, passing from 18 at 220 GPa to 7 at 420 GPa. In addition, we consider the dynamical screening, $-\mathrm{Im}\,\epsilon^{-1}(\mathbf{q}, \omega)$, which can be measured by electron-energy loss spectroscopy (EELS) or inelastic x-ray scattering and which we calculated in time-dependent LDA [21] (with the inclusion of 40 bands). The EELS spectrum, for each momentum transfer $\mathbf{q}$ (either along the c axis or in the perpendicular ab plane), is characterized by a main structure, which corresponds to the frequency of the collective oscillations of the valence electrons in the system, i.e., plasmons (Fig. 3). These plasmon structures show a small dispersion with the momentum transfer $\mathbf{q}$ (see Ref. [15], Fig. 6). While detailed features depend on band structure properties, in this case the Drude model is still partially able to track the dependence of the plasmon frequency ω_p with the compression. According to the Drude model, the plasmon frequency increases linearly with the square root of the density [1]: $\omega_p = \sqrt{4\pi\rho}$. Using this formula at the densities corresponding to the three considered pressures, we have $\omega_p = 13.5$, 14.6, and 15.4 eV (grey arrows in Fig. 3) when we consider only 4 valence electrons in the unit cell. In a way, this corresponds to a definition of ''valence'' electrons in this extreme situation where the usual view of electrons belonging to a particular atom is no longer strictly valid. Being based on a uniform electron

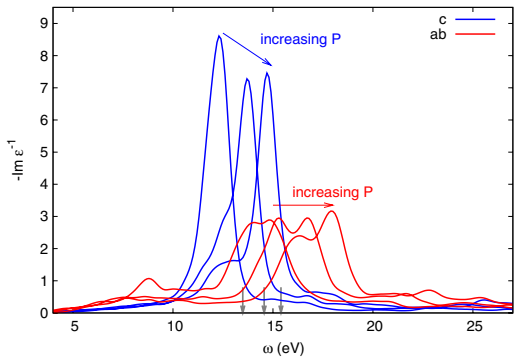

FIG. 3 (color online). EELS spectra along the two polarizations for **q** equal to 0.1 reciprocal lattice units at 220, 320, and 420 GPa. The grey arrows at the bottom of the figure mark the corresponding Drude plasmon energies (see text).

gas, the Drude model describes an average behavior of the dielectric response of the system, but is obviously not able to catch its anisotropy, which leads to the splitting between the plasmons along the *c* axis and in the perpendicular plane (the Drude plasmon energy falls somewhat in the middle). Moreover, at low pressures another smaller plasmonic structure appears only in the in-plane direction at about 8 eV, which is strongly suppressed by increasing the applied pressure (see Ref. [15], Fig. 7). Both the anisotropy in the lattice structure and the higher-energy localization of the spectral weight for the in-plane polarization (see Ref. [15], Fig. 7) contribute in the same way to the splitting of the plasmon energies in the two directions.

In conclusion, our first-principle predictions for both absorption and EELS spectra can indeed be used to confirm the crystal structure of this phase of dense transparent sodium. First of all, since the binding energy of the bound exciton is of the order of a hundred meV, our results for the optical spectra support the hypothesis of Ma *et al.* [5], which was based only on ground-state and band gap calculations. Moreover, even though ground-state calculations overestimate the pressure value at which the transition to the *hP*4 phase occurs [5], our predictions for the optical properties are not biased by this error. In fact, while excitonic effects are varying with the applied pressure (and can be influenced by the temperature as well [22]), from our analysis it turns out that key features of the spectra, like the polarization anisotropy, are essentially linked to the symmetry of the crystal structure and can be observed in a very large range of pressure (see Ref. [15], Fig. 4). This also implies that sodium becomes transparent in the visible range at a lower pressure in one polarization direction while still being "metallic" in the other. Therefore we suggest the measurement of the spectra along the two polarizations as the key test to verify conclusively that transparent sodium crystallizes in the *hP*4 structure. Photoluminescence would put into evidence the nature of the predicted bound exciton which has a low oscillator strength in optics.

We acknowledge fruitful discussions with G. Vignale and F. Sottile and thank the authors of Ref. [5] for sending their relaxed geometries which are used in the present work. This work was supported by the Spanish MEC (FIS2007-65702-C02-01), "Grupos Consolidados UPV/EHU del Gobierno Vasco" (IT-319-07), and the European Union through the e-I3 ETSF project (Contract No. 211956). We acknowledge support by the Barcelona Supercomputing Center, "Red Espanola de Supercomputacion." We have used ABINIT [23], DP, and EXC codes [24].

[1] G. Grosso and G. Pastori-Parravicini, *Solid State Physics* (Academic, New York, 2000).
[2] M. I. McMahon *et al.*, Proc. Natl. Acad. Sci. U.S.A. **104**, 17297 (2007).
[3] E. Gregoryanz *et al.*, Science **320**, 1054 (2008).
[4] E. Gregoryanz *et al.*, Phys. Rev. Lett. **94**, 185502 (2005).
[5] Y. Ma *et al.*, Nature (London) **458**, 182 (2009).
[6] L. F. Lundegaard *et al.*, Phys. Rev. B **79**, 064105 (2009).
[7] A. Lazicki *et al.*, Proc. Natl. Acad. Sci. U.S.A. **106**, 6525 (2009).
[8] J.-Y. Raty, E. Schwegler, and S. A. Bonev, Nature (London) **449**, 448 (2007).
[9] J. B. Neaton and N. W. Ashcroft, Phys. Rev. Lett. **86**, 2830 (2001).
[10] N. E. Christensen and D. L. Novikov, Solid State Commun. **119**, 477 (2001).
[11] B. Rousseau and N. W. Ashcroft, Phys. Rev. Lett. **101**, 046407 (2008).
[12] N. W. Ashcroft, Nature (London) **458**, 158 (2009); Proc. Natl. Acad. Sci. U.S.A. **105**, 5 (2008).
[13] G. Onida, L. Reining, and A. Rubio, Rev. Mod. Phys. **74**, 601 (2002), and references therein.
[14] L. Hedin, Phys. Rev. **139**, A796 (1965).
[15] See supplementary material at http://link.aps.org/supplemental/10.1103/PhysRevLett.104.216404 for additional figures.
[16] R. W. Godby and R. J. Needs, Phys. Rev. Lett. **62**, 1169 (1989).
[17] We use 1024 **k** points and 0.3 eV broadening when we study the dependence on pressure of the optical spectra. For the plot of the exciton wave function the **k** point grid includes the Γ point.
[18] P. Abbamonte *et al.*, Proc. Natl. Acad. Sci. U.S.A. **105**, 12159 (2008).
[19] J. L. Dye, Science **247**, 663 (1990).
[20] S. L. Adler, Phys. Rev. **126**, 413 (1962); N. Wiser, Phys. Rev. **129**, 62 (1963).
[21] H.-C. Weissker *et al.*, Phys. Rev. Lett. **97**, 237602 (2006).
[22] A. Marini, Phys. Rev. Lett. **101**, 106405 (2008).
[23] X. Gonze *et al.*, Z. Kristallogr. **220**, 558 (2005).
[24] The DP and EXC codes are developed by the French node of the ETSF; see http://etsf.polytechnique.fr/Software.